

Numerical Simulation of Wind Turbine Blade-Tower Interaction

Qiang Wang, Hu Zhou and Decheng Wan*

*State Key Laboratory of Ocean Engineering, School of Naval Architecture and Ocean Engineering,
Shanghai Jiao Tong University, Shanghai 200240, China*

Abstract: Numerical simulations of wind turbine blade-tower interaction by using the open source OpenFOAM tools coupled with arbitrary mesh interface (AMI) method were presented. The governing equations were the unsteady Reynolds-averaged Navier-Stokes (RANS) which were solved by the pimpleDyMFoam solver, and the AMI method was employed to handle mesh movements. The National Renewable Energy Laboratory (NREL) phase VI wind turbine in upwind configuration was selected for numerical tests with different incoming wind speeds (5, 10, 15, and 25 m/s) at a fixed blade pitch and constant rotational speed. Detailed numerical results of vortex structure, time histories of thrust, and pressure distribution on the blade and tower were presented. The findings show that the wind turbine tower has little effect on the whole aerodynamic performance of an upwind wind turbine, while the rotating rotor will induce an obvious cyclic drop in the front pressure of the tower. Also, strong interaction of blade tip vortices with separation from the tower was observed.

Keywords: NREL phase VI, wind turbine, pimpleDyMFoam, arbitrary mesh interface (AMI), blade-tower interaction

Article ID: 1671-9433(2012)03-0321-07

1 Introduction

Wind energy is a kind of renewable energy that is clean, relatively cheap, and enjoys great generation potential; as a result, it is now being developed all over the world. The generation potential of wind power for on land and near-shore areas is estimated at 72TW, which is more than five times of the world's current energy consumption (Archer and Jacobson, 2005). The horizontal axis upwind wind turbine is the most popular method to capture wind energy. However, complex flows around the wind turbine always result in its unstable and unexpected aerodynamic performance. Therefore, in order to design more efficient and reliable wind turbines, a thorough understanding of the flows around them along with their aerodynamic behavior are of critical significance. The rotor diameter of wind turbines has become much larger, from 15 m in 1985 to 126m in 2009 (EWEA, 2010), and may reach 170 m by 2013 (EWEA, 2011). This results in more complex flows for modern turbines and more elastic blades, making blade-tower interaction an important factor to consider.

Most numerical computations of wind turbines are compared to the National Renewable Energy Laboratory (NREL) Unsteady Aerodynamics Experiment (UAE) carried out in the NASA Ames 24.4 m×36.6 m wind tunnel in 1999 (Hand *et al.*, 2001). The most important results come from Phase VI of the experiments which is regarded as a

benchmark for evaluation of wind turbine aerodynamics computer codes. Extensive studies on aerodynamic performance of wind turbine rotors have been carried out using computational fluid dynamics (CFD) (Sørensen *et al.*, 2002; Johansen *et al.*, 2002; Duque *et al.*, 2003; Potsdam and Mavriplis, 2009). These works show that CFD can accurately predict aerodynamic performance of wind turbine rotors and capture the complex flows, justifying the use of CFD codes in more complex blade-tower interaction problems. Most researchers have studied the blade-tower interaction in a downwind wind turbine. Duque *et al.* (1999) was the first to perform CFD calculation of a complete downwind wind turbine. The work was based on an unsteady compressible thin-layer Navier-Stokes solver using overset grids methods. However, the blade-tower wake interaction was smaller in duration and amplitude in comparison to the experiment. Zahle *et al.* (2009) studied downwind rotor-tower interaction using the finite volume flow solver EllipSys3D with overset grids on a NREL phase VI wind turbine. The calculation showed satisfactory agreement with experimental results, and the detailed features of the flows were captured. However, some deviation was seen at a high wind speed. For upwind configuration, Gomez-Iradi and Steijl (2009) was the first to perform CFD calculation. The work was carried out using a compressible Navier-Stokes CFD code Wind MultiBlock (WMB) with multiblock grids on the NREL phase VI wind turbine. The computation showed good agreement with experimental results. However, only a 7 m/s wind speed case was studied. Li *et al.* (2012) studied the NREL phase VI wind turbine using incompressible RANS and DES solver CFIowa-ship v4.5 with overset grids. Their results showed satisfactory agreement with experimental results,

Received date: 2012-06-11.

Foundation item: Supported by the National Natural Science Foundation of China under Grant Nos.50739004 and 11072154.

*Corresponding author: dcwan@sjtu.edu.cn

© Harbin Engineering University and Springer-Verlag Berlin Heidelberg 2012

but the work focused on aerodynamic performance and only a few results of blade-tower interaction were obtained.

The objective of this paper is to do an extensive study of the blade-tower interaction of the NREL phase VI wind turbine in upwind configuration. This work is among the first to use the OpenFOAM method to simulate the interaction between blade and tower, and is also among the first to handle mesh rotating movements with arbitrary mesh interface (AMI) technology. In comparison with previous simulations, more detailed and comprehensive results are obtained. Computations for the turbine include four wind speeds (5, 10, 15, and 25 m/s) at a fixed blade pitch angle of 3° with a constant rotational speed of 72 r/min. Numerical results including vortical structure, time histories of thrust and pressure distribution on the blade and tower are analyzed.

2 Numerical methods

OpenFOAM (Jasak *et al.*, 2007), short for open field operation and manipulation, is an open source object-oriented library for numerical simulations in continuum mechanics written in C++. The library provides Finite Volume discretization in an operator form and with polyhedral mesh support, with relevant auxiliary tools and support for massively parallel computing. OpenFOAM is gaining considerable popularity in academic research and among industrial users. The group led by Professor Decheng Wan at the School of Naval Architecture and Ocean Engineering of Shanghai Jiao Tong University has done much work on developing and using OpenFOAM. Cha and Wan (2011) and Cao (2011) developed a numerical wave tank based on the solver *interDyMFOam* and did a lot of work on wave run-up on a cylinder. (Shen and Wan, 2012) implanted a six-degrees-of-freedom (6DOF) module into the wave tank and developed the code *naoe-FOAM-SJTU*, which is able to simulate motions and dynamic response of ships and platforms in waves.

This paper is based on an unsteady incompressible RANS solver-*pimpleDyMFOam* with an AMI method (released with OpenFOAM-2.1.0) to handle mesh movements. The principle of Arbitrary Mesh Interface is much like the general grid interface (GGI) (Beaudoin and Jasak, 2008). It is based on a set of weighting factors to properly balance the flux at the AMI interface. The PIMPLE algorithm (Jasak, 1996) (hybrid pressure implicit with splitting of operators (PISO) and semi-implicit method for pressure-linked equations (SIMPLE)) is adopted in the solver to solve the pressure velocity coupling. Convection terms are discretized with second-order head wind and with a second-order centered scheme for the viscous term. The temporal terms are discretized using a second-order Euler implicit scheme. The $k-\omega$ shear stress transport (SST) model (Menter, 1994; Menter, 2009) turbulence model with wall functions is adopted for modeling turbulence in the boundary layer.

3 Wind turbine model and mesh strategy

The testing wind turbine is the NREL phase VI, which has a power of 20 kW. It has two blades with a NREL S809 profile. The rotor diameter is 10.058 m and the hub height is 12.192m. Detailed data can be found in the report (Hand *et al.*, 2001). The computation domain is set as follows: 5 m from inlet to the turbine, 20 m from the turbine to outlet, and 15 m from the turbine to the sides. The origin of coordinates is at the center of rotation of the turbine. The background mesh is built with ANSYS ICEM-CFD software using O-O-type blocks; the inner side of the O-type block is used to ensure the mesh quality of the AMI faces. Mesh in the center is designed to be close to cubic, and the region should cover the whole rotor to correctly capture the geometry. In the x direction, mesh is refined in the region $[-0.8\text{ m}, 0.8\text{ m}]$ to the size of around $0.1\text{ m} \times 0.2\text{ m} \times 0.2\text{ m}$ and in $[0.8\text{ m}, 5\text{ m}]$ to the size of $0.2\text{ m} \times 0.2\text{ m}$. The cell number of the background mesh is around 255 000. Then the *snappyHexMesh* utility (mesh tool in OpenFOAM) is used to create the final mesh. The surface refinement level is 3 and feature refinement level is 4 with 3 mesh layers to keep $30 < y+ < 300$. The final mesh is shown in Fig. 1.

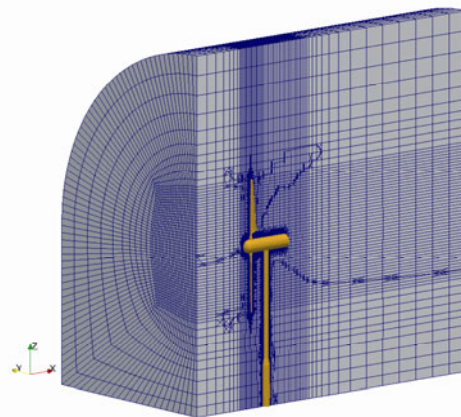


Fig. 1 Mesh overview

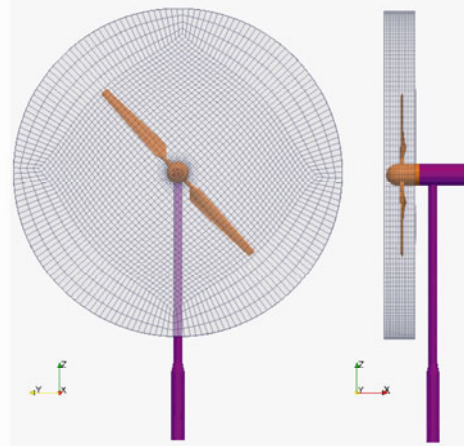


Fig. 2 Mesh of AMI region

After this work, other OpenFOAM utilities such as topoSet are used to create the AMI region, as shown in Fig. 2, which is a cylindrical region with a radius of 7.5 m, the front face being 0.8 m away from the origin and the back face 0.6 m away from the origin.

Sequence S of NREL experiments is chosen in this paper. Computations for this sequence include the upwind configuration at four wind speeds (5, 10, 15, and 25 m/s) with a fixed blade pitch angle of 3° and constant rotational speed of 72 r/min. The detailed setup is shown in Table 1.

Table 1 Computation cases

Run	Wind speed (m·s ⁻¹)	Density (kg·m ⁻³)	Kinematic viscosity (m ² ·s ⁻¹)	Pitch/(°)
S0500000	5	1.243	1.424E-5	3
S1000000	10	1.246	1.423E-5	3
S1500000	15	1.224	1.450E-5	3
S2500001	25	1.220	1.454E-5	3

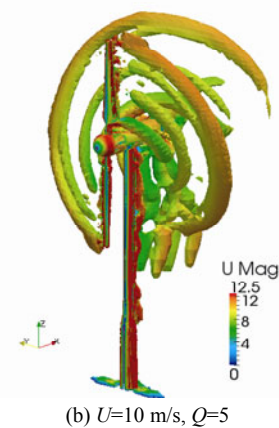
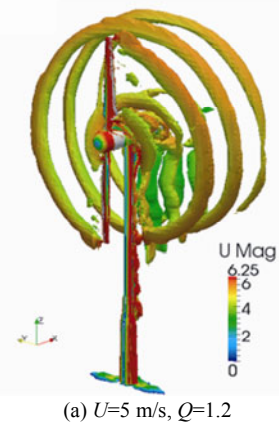
4 Results and discussions

The authors of this paper have already completed the calculation of flows and aerodynamic performance of the NREL phase VI rotor-only model (Zhou *et al.*, 2012) with the same case as set up in this paper. An extensive comparison with experiments shows good agreement (Zhou *et al.*, 2012), which indicates the great potential of the pimpleDyMFoam code. In this paper, some results are compared to the rotor-only model to study the differences between the two models. At the same time, the results in this paper are confirmed by the verification of the convergence of mesh.

4.1 Vortex structure

The vortex structure for the four wind speeds is shown in Fig. 3. Vortices are colored using the second invariant of the velocity gradient tensor (Hunt *et al.*, 1988) at $Q=1.2, 5, 12,$ and 30 as the wind speed increases. It is clear that at 5 m/s and 10 m/s, flows around blades are almost attached, with development of blade flow separation at 10 m/s. Strong and stable blade tip vortices are observed at these two wind speeds, especially at 5 m/s. Additionally, strong vortices detached from the blade root are seen, where the geometry changes quickly from a cylinder to S809 airfoil. At 15 m/s, most of the blade suffers unsteady separation while at 25m/s almost the whole trailing edge of blade experiences a massive flow separation. Notice that all the vortical structures dissipate quickly after moving about one blade length away from the wind turbine, where mesh refinement is covered. So a longer region of refinement is needed if one wants to obtain a longer vortical structure, but it will no doubt increase the computation cost. In addition, for the two higher wind speeds, the interaction of the blade tip vortices with the separation from blades changes the shape of the

blade tip vortices, most obviously at 15 m/s. A more obvious interaction is between the blade tip vortices and vortices detached from the tower, especially at 10 m/s and 15 m/s. The interaction changes the shape and also causes breakdown of tower vortices. It is also noticed that tower vortices are only obvious on the upper half of the tower; this is a result of coarse mesh at the lower part of the tower, as shown in Fig. 1. In order to obtain an insight view of the interaction between blade tip vortices and tower vortices, a cut plane at $r/R=0.95$ which equals $z=-4.78$ m at 10 m/s at three times (2.275, 2.35, and 2.425 s) is shown in Fig. 4. The background shows the velocity field while the iso-surface of Q is shown above, also colored by Q . From the velocity field, it is clear that the tower causes velocity reduction, and the velocity field after the tower shows wave-like periodic fluctuations. Vortical structure at 2.27 s shows periodic vortices detaching, forming the classical Kármán vortex street. At this moment, the cut plane captured two large vortices which are cut from the blade tip vortices. The upper one has already connected to tower vortices. At 2.35 s, both the upper and lower blade tip vortices are connected to tower vortices. The interaction also changes the shape of the tower vortices. At 2.425 s, the blades tip vortices and the tower vortices are finally integrated; the interaction changes the shape of these vortices and swallows the tower vortices. The figure also clearly shows the dissipation of vortices on a coarser mesh.



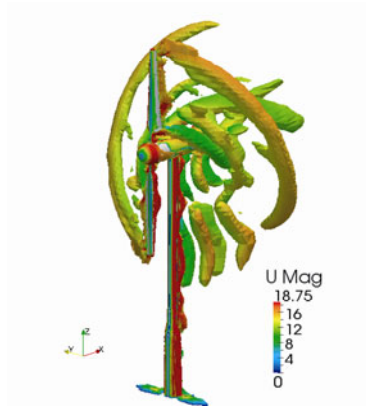
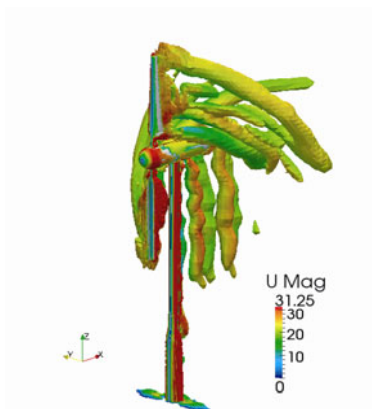
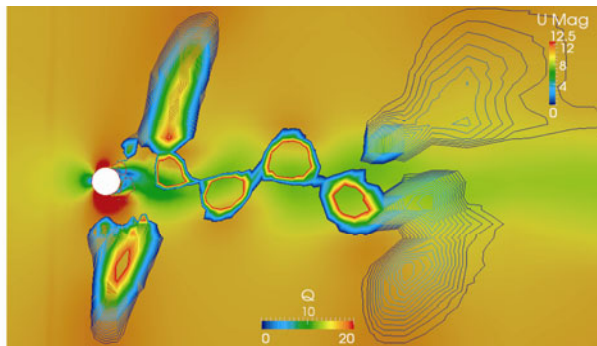
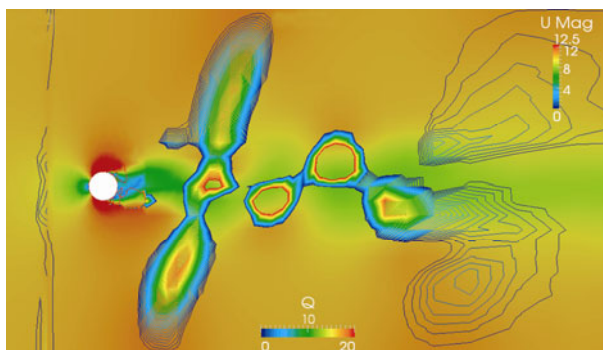
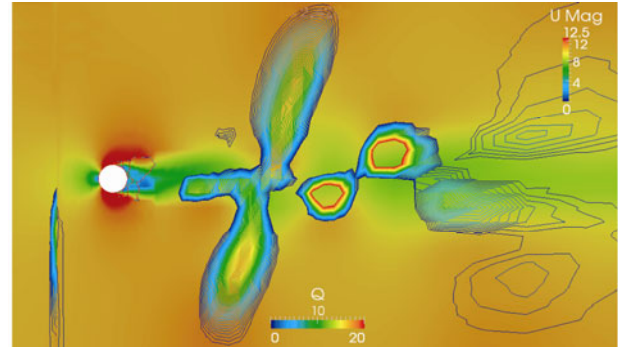
(c) $U=15$ m/s, $Q=12$ (d) $U=25$ m/s, $Q=30$

Fig. 3 Vortex structure at different wind speeds

(a) $t=2.275$ s(b) $t=2.35$ s(c) $t=2.425$ sFig. 4 Blade tip vortices and tower vortices interaction at three times (cut plane at $r/R=0.95$)

4.2 Aerodynamic performance

The interaction between blade and tower vortices will impact the aerodynamic performance of the wind turbine in the long term. The simulation time selected is 2.6 s, and it can be seen from Fig. 5 that the thrust of the rotor-only model at 15 m/s and 25 m/s is almost constant after 0.5 s. So it is reasonable to choose 2.6 s as the simulation time. Time histories of thrust at 5, 10, 15, and 25 m/s are shown in Fig. 6. The blue dotted line shows the results from the rotor-only model (Zhou *et al.*, 2012). In order to compare fairly, the thrust of one blade is multiplied by two instead of adding up the thrust of two blades, which may smooth the transient behavior since the two blades have different instantaneous thrusts. Compared to the rotor-only model, the impact of blade-tower interaction on thrust is very clear. For all the four wind speeds, the thrust suffers a drop when the azimuthal angle approaches 180 degrees and the thrust is recovered when the azimuthal angle passes 180 degrees, while for the rotor-only model, the thrust maintains a relatively stable value throughout the cycle. However, the reduction of thrust only enjoys a small percentage of the total thrust. In addition, the percentage drops when wind speed increases about 9% at 5 m/s, 6% at 10 m/s, and reduces to 4% and 2% when it comes to 15 m/s and 25 m/s. This indicates that the increase of amplitude of thrust reduction is less than that of thrust itself due to the increase of wind speed. Besides, the reduction influences only about 1/6 of the revolution for the wind turbine. Therefore, it can be concluded that for upwind wind turbines, thrust reduction due to blade-tower interaction is small. But the cyclic reduction should introduce vibration at a certain frequency (related to RPM), which should be deviated from the natural frequency of other components to avoid resonance.

As thrust is integrated over the blade, evaluation of local pressure coefficient distribution allows a more detailed check of the influence of the tower on the aerodynamic performance of a wind turbine. The pressure coefficient distributions at five sections ($r/R=0.3$, $r/R=0.47$, $r/R=0.63$, $r/R=0.8$, and $r/R=0.95$) for 5 m/s and 10 m/s are shown in Fig. 7. For the whole turbine model, the pressure distribution is calculated at an azimuthal angle of 180 degrees. The figure shows no significant deviation of

pressure distributions for the two models; the curves are almost identical at 5 m/s. At 10 m/s a small reduction of the pressure coefficient is observed at the suction side of the blade, which results in thrust reduction. This fact proves the previous claim that the influence of the tower on the aerodynamic performance of a wind turbine is small.

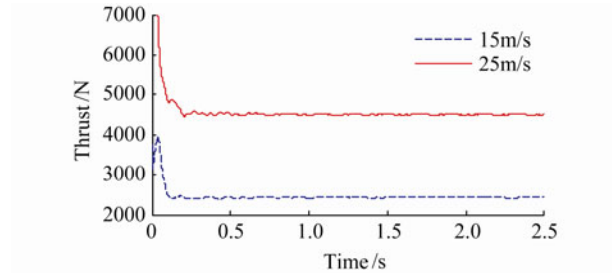


Fig. 5 Time histories of thrust of rotor at 15 m/s and 25 m/s

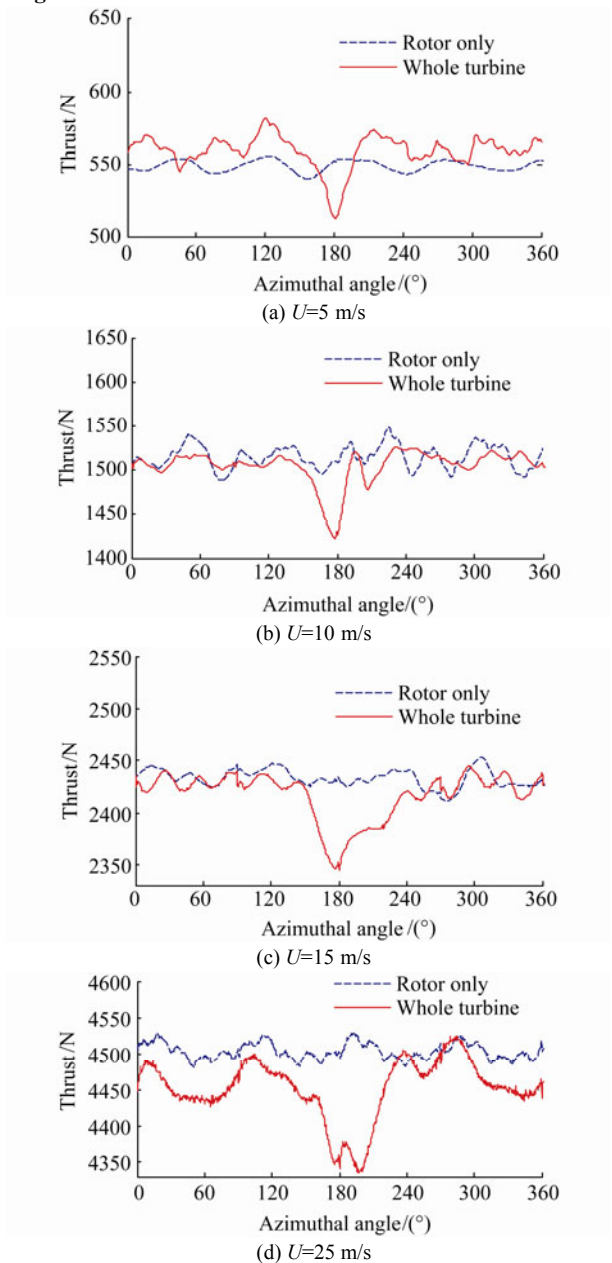


Fig. 6 Time histories of thrust for different wind speeds

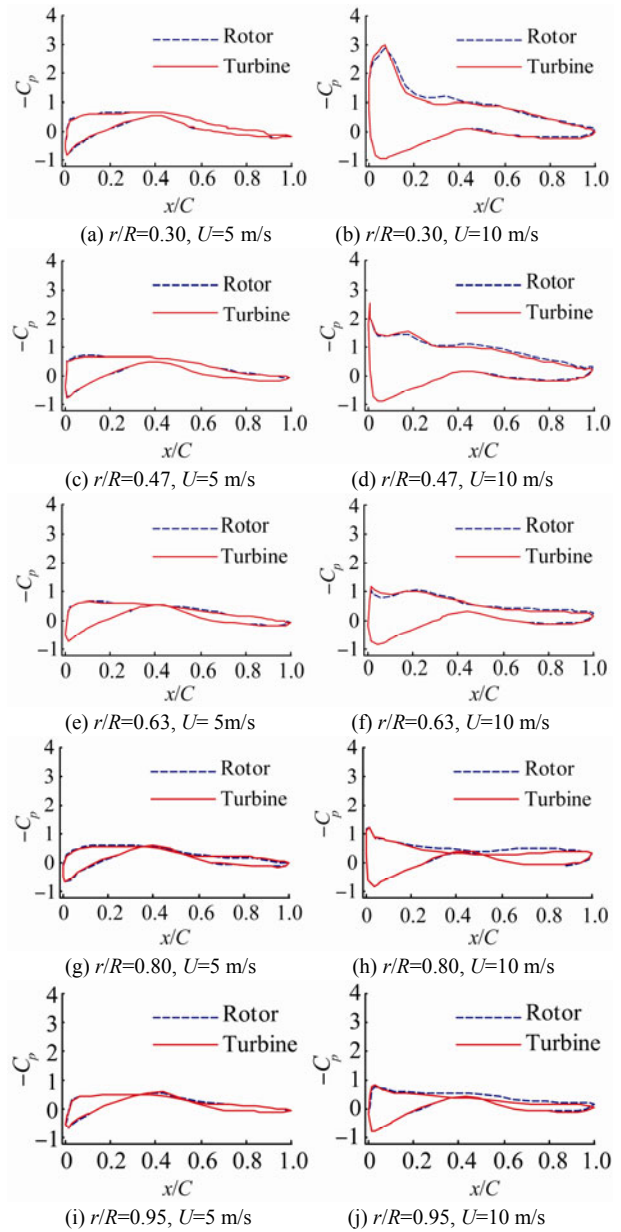
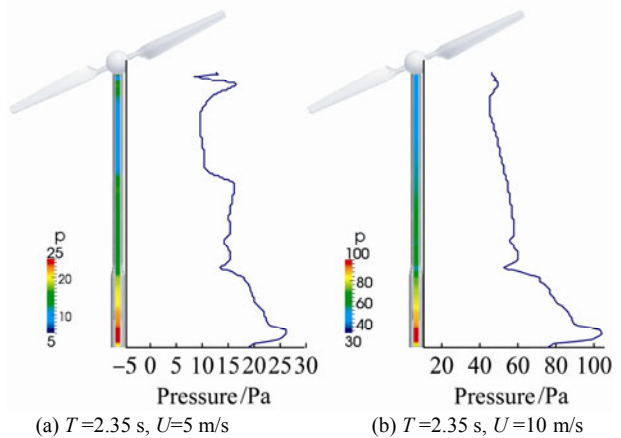


Fig. 7 Pressure coefficient distribution for 5 and 10 m/s at five sections



(a) $T=2.35$ s, $U=5$ m/s

(b) $T=2.35$ s, $U=10$ m/s

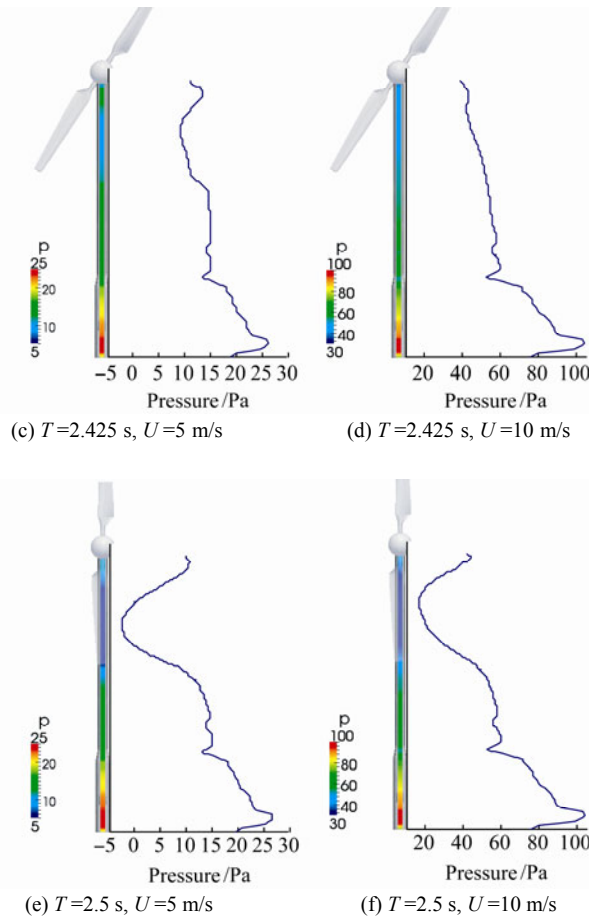


Fig. 8 Tower pressure distribution for 5 and 10 m/s at different times

4.3 Tower pressure distribution

The previous part of the paper mainly discussed the influence of a tower on a blade. This part will investigate the impact of blade on tower. The tower pressure distributions at a leading edge for 5 m/s and 10 m/s at three different time (2.35, 2.425, and 2.5 s) are shown in Fig. 8. The influence of the rotating blade on tower pressure distribution mainly exists within the blade swept area; tower pressure outside this area stays unchanged. At 5 m/s, the effect of tower never disappears. Even at 2.35 s when there is over 60 degree between blade and tower, an obvious drop of tower pressure within the swept area is observed. This phenomenon was also obtained by Gomez-Irardi and Steijl (2009). However, at 10 m/s this effect is much weaker than that at 5 m/s. Both of the two conditions suffer a huge drop of tower pressure within the swept area when the azimuthal angle reaches 180 degree. This is very dangerous in real life, since the huge drop in pressure will result in deformation of the blade toward the tower, which can cause collision.

5 Conclusions

Numerical simulations of the blade-tower interaction of a NREL phase VI wind turbine in upwind configurations were presented. The simulations were performed using the

unsteady RANS solver pimpleDyMFOam with an Arbitrary Mesh Interface to handle mesh movements. Computations for the turbine include four wind speeds (5, 10, 15, and 25 m/s) at a fixed blade pitch angle of 3° with a constant rotational speed 72 r/min. Detailed investigation on the vortex structure clearly presents the process of interaction of blade tip vortices and tower vortices. The simulation of the process of interaction will help to deepen the understanding of the mechanism of blade-tower interaction. Comparison of time histories of thrust and pressure distribution with a rotor-only model shows a little difference which indicates that the influence of the tower on the aerodynamic performance of a wind turbine is small. A study of tower pressure distribution shows that the tower pressure will suffer a huge drop when the blade covers the tower which may cause collision. Additionally, the effect of the blade on the tower pressure obviously exists throughout the revolution at 5 m/s, which is not the case at 10 m/s. The numerical results show that the tower has little effect on the whole aerodynamic performance of an upwind wind turbine while the rotating rotor will induce an obvious cyclic drop of the front pressure of the tower. Strong interaction of blade tip vortices with separation from the blade and tower was observed. The presented numerical approach in dealing with complex flows of a wind turbine was validated by the presented numerical test, which lays a solid foundation for further research in areas such as floating offshore wind turbines, and provides a valuable guide for wind turbine design.

Acknowledgement

The experimental data was provided by Dr. Scott Schreck from the National Renewable Energy Laboratory. His support is highly appreciated. This work is supported by the National Natural Science Foundation of China (Grant Nos. 50739004 and 11072154), Foundation of State Key Laboratory of Ocean Engineering of China (GKZD 010053-11), the Program for Professors of Special Appointment (Eastern Scholar) at Shanghai Institutions of Higher Learning (2008007), and The Lloyd's Register Educational Trust (The LRET) through the joint center involving University College London, Shanghai Jiao Tong University, and Harbin Engineering University, to which the authors are most grateful.

References

- Archer CL, Jacobson MZ (2005). Evaluation of global wind power. *J. Geophys. Res.*, **110**(43), D12110.
- Beaudoin M, Jasak H (2008). Development of a generalized grid interface for turbomachinery simulations with OpenFOAM. *Open Source CFD International Conference*, Berlin, Germany, 4-5.
- Cha JJ, Wan DC (2011). Numerical wave generation and absorption based on OpenFOAM. *Chinese Ocean Engineering*, **29**(3), 1-12.
- Cao HJ, Cha JJ, Wan DC (2011). Numerical simulation of wave

- run-up around a vertical cylinder. *Proceedings of the 21st International Offshore and Polar Engineering Conference*, Maui, Hawaii, USA, 726.
- Duque EPN, Burkland MD, Johnson W (2003). Navier-Stokes and comprehensive analysis performance predictions of the NREL phase VI experiment. *Journal of Solar Energy Engineering*, **125**(4), 457-467.
- Duque EPN, Van Dam C, Hughes S (1999). Navier-Stokes simulations of the NREL combined experiment phase II rotor. *Proceedings of the 18th ASME Wind Energy Symposium*, Reno, AIAA-99-0037.
- EWEA (2010). Wind energy factsheets. European Wind Energy Association.
- EWEA (2011). Wind in our sails. European Wind Energy Association.
- Gomez-Iradi S, Steijl R (2009). Development and validation of a CFD technique for the aerodynamic analysis of HAWT. *Journal of Solar Energy Engineering*, **131**(8), 031009.1-031009.13.
- Hand MM, Simms DA, Fingersh LJ, Jager DW, Cotrell JR, Schreck S, Larwood SM (2001). Unsteady aerodynamics experiment phase VI: Wind tunnel test configurations and available data campaigns. National Renewable Energy Laboratory, Lakewood. Technical report, NREL/TP-500-29955.
- Hunt J, Wray A, Moin P (1988). Eddies, streams, and convergence zones in turbulent flows. *Center for Turbulence Research Report*, CTR-S88, 193-208.
- Jasak H (1996). Error analysis and estimation for the finite volume method with applications to fluid flows. PhD thesis, Imperial College, University of London, London.
- Jasak H, Jemcov A, Tukovic Z (2007). Openfoam: A C++ library for complex physics simulations. *International Workshop on Coupled Methods in Numerical Dynamics*, Dubrovnik, Croatia, 1-20.
- Johansen J, Sørensen N, Michelsen J, Schreck S (2002). Detached-eddy simulation of flow around the NREL Phase VI blade. *Wind Energy*, **5**(2/3), 185-197.
- Li YW, Paik KJ, Xing T, Carrica PM (2012). Dynamic overset CFD simulations of wind turbine aerodynamics. *Renewable Energy*, **37**(1), 285-298.
- Menter FR (1994). Two-equation eddy-viscosity turbulence models for engineering applications. *AIAA Journal*, **32**(8), 1598-1605.
- Menter FR (2009). Review of the shear-stress transport turbulence model experience from an industrial perspective. *International Journal of Computational Fluid Dynamics*, **23**(4), 305-316.
- Potsdam MA, Mavriplis DJ (2009). Unstructured mesh CFD aerodynamic analysis of the NREL Phase VI rotor. *47th AIAA Aerospace Sciences Meeting*, Orlando, Florida.
- Shen ZR, Wan DC (2012). RANS computations of added resistance and motions of ship inhead waves. *Proceedings of the Twenty-second International Offshore and Pollarding Conference (ISOPE)*, Rhodes, Greece, 1096-1103.
- Sørensen N, Michelsen J, Schreck S (2002). Navier-Stokes predictions of the NREL phase VI rotor in the NASA Ames 80ft×120ft wind tunnel. *Wind Energy*, **5**(2/3), 151-169.
- Zahle F, Sørensen NN, Johansen J (2009). Wind turbine rotor - tower interaction using an incompressible overset grid method. *Wind Energy*, **12**(6), 594-619.
- Zhou H, Wang Q, Wan DC (2012). Numerical simulations of the 3D viscous flows around wind turbine blade. *Proceedings of 21st National Conference of Hydrodynamics*. (in Chinese, in press).



Qiang Wang has recently obtained the Bachelor's Degree of Science in Engineering (Naval Architecture and Ocean Engineering) from Shanghai Jiao Tong University. He has extensive research interest on marine renewable energy and hydrodynamics.
wangqiangele@gmail.com



Hu Zhou is a graduate student in School of Naval Architecture and Ocean Engineering in Shanghai Jiao Tong University. The field of research is offshore wind turbine and CFD.
zhouhu@sjtu.edu.cn



Decheng Wan is a professor of School of Naval Architecture, Ocean and Civil Engineering, Shanghai Jiao Tong University, and a distinguished professor of Shanghai Eastern Scholar. His research interests include marine hydrodynamics and computational fluid dynamics, marine numerical wave tank, nonlinear wave theory, fluid-structure interaction, and high performance computation on complex flows, etc.